American Mineralogist, Volume 90, pages 240–246, 2005

The role of water in the structures of synthetic hallimondite, $Pb_2[(UO_2)(AsO_4)_2](H_2O)_n$ and synthetic parsonsite, $Pb_2[(UO_2)(PO_4)_2](H_2O)_n$, $0 \le n \le 0.5$

ANDREW J. LOCOCK,[1,*] PETER C. BURNS,[2] AND THEODORE M. FLYNN[3]

[1]Mineralogy, Department of Natural History, Royal Ontario Museum, 100 Queen's Park, Toronto, Ontario, M5S 2C6, Canada
[2]Department of Civil Engineering and Geological Sciences, University of Notre Dame, 156 Fitzpatrick Hall, Notre Dame, Indiana 46556, U.S.A.
[3]Department of Geology, University of Illinois, Urbana-Champaign, Illinois 61801, U.S.A.

ABSTRACT

The crystal structures of synthetic hallimondite and synthetic parsonsite have been refined by full-matrix least-squares techniques to agreement indices (hallimondite, parsonsite) wR_2 of 5.5, and 7.6% for all data, and $R1$ of 2.7 and 3.4%, calculated for 3391 and 3181 unique observed reflections ($|F_o| \ge 4\sigma_F$), respectively. Hallimondite is triclinic, space group $P\bar{1}$, $Z = 2$, $a = 7.1153(8)$, $b = 10.4780(12)$, $c = 6.8571(8)$ Å, $\alpha = 101.178(3)°$, $\beta = 95.711(3)°$, $\gamma = 86.651(3)°$, $V = 498.64(3)$ Å^3, and is isostructural with parsonsite, triclinic, space group $P\bar{1}$, $Z = 2$, $a = 6.8432(5)$, $b = 10.4105(7)$, $c = 6.6718(4)$ Å, $\alpha = 101.418(1)°$, $\beta = 98.347(2)°$, $\gamma = 86.264(2)°$, $V = 460.64(5)$ Å^3. In both structures, hexavalent uranium occurs as a uranyl pentagonal bipyramid. The uranyl polyhedra share an edge, forming dimers that are linked by edge- and vertex-sharing with arsenate or phosphate tetrahedra to form chains along [001]. Two symmetrically distinct Pb positions connect the chains. In hallimondite, a partially occupied oxygen atom is located in the cavity between the uranyl arsenate chains and Pb positions, and is attributed to an H_2O group. The crystal of synthetic parsonsite investigated does not have appreciable electron density at this position, but its structural cavity is large enough to contain H_2O. The presence of H_2O in synthetic hallimondite, and its absence in synthetic parsonsite, are supported by the results of FTIR spectroscopy. In conjunction with thermogravimetric results from the literature, we suggest that the formula of parsonsite should be considered $Pb_2[(UO_2)(PO_4)_2](H_2O)_n$, and hallimondite, $Pb_2[(UO_2)(AsO_4)_2](H_2O)_n$, with $0 \le n \le 0.5$ in each case.

INTRODUCTION

The crystal chemistry of hexavalent uranium has attracted considerable attention in recent years (Burns et al. 1996, 1997; Burns 1999; King 2002). Four major structural classes of inorganic uranyl phosphates and uranyl arsenates have been recognized: (1) structures containing the autunite-type sheet (autunite and meta-autunite groups), (2) structures containing the phosphuranylite-type sheet (phosphuranylite group), (3) structures containing the uranophane sheet-anion topology, and (4) chain structures. Sheets of polyhedra dominate the structures of uranyl phosphates and arsenates. The autunite sheet involves the sharing of vertices between uranyl square bipyramids and phosphate or arsenate tetrahedra. The phosphuranylite sheet contains uranyl pentagonal and hexagonal bipyramids that share edges to form chains that are cross-linked by sharing vertices and edges with phosphate or arsenate tetrahedra. In some cases, sheets in minerals of the phosphuranylite group are linked by bonds to U^{6+} in the interlayer, resulting in framework structures. The uranophane-type sheet that involves chains of edge-sharing uranyl pentagonal bipyramids linked by sharing edges and vertices with tetrahedra has been found in only a few inorganic uranyl phosphates and uranyl arsenates, and in uranyl phosphate or arsenate minerals is only represented by ulrichite, $Cu[Ca(H_2O)_2(UO_2)(PO_4)_2](H_2O)_2$ (Kolitsch and Giester 2001), and the mixed arsenate-arsenite seelite, $Mg(UO_2)_2(AsO_3)_{1.4}(AsO_4)_{0.6}(H_2O)_7$ (Piret and Piret-Meunier 1994).

Chain structures are relatively uncommon in uranyl phosphate or arsenate minerals, and occur only in walpurgite, $(UO_2)Bi_4O_4(AsO_4)_2(H_2O)_2$ (Mereiter 1982), orthowalpurgite, $(UO_2)Bi_4O_4(AsO_4)_2(H_2O)_2$ (Krause et al. 1995), and parsonsite, $Pb_2[(UO_2)(PO_4)_2]$ (Burns 2000). The structures of the phosphate analogue of walpurgite, IMA2001-062, $(UO_2)Bi_4O_4(PO_4)_2(H_2O)_2$, and of the arsenate analogue of parsonsite, hallimondite, $Pb_2[(UO_2)(AsO_4)_2]$ (Walenta 1965) have not been reported previously. As part of our ongoing research into the structures of uranyl phosphates and arsenates, we have synthesized hallimondite and parsonsite, and herein present the structure of hallimondite and a new refinement of parsonsite.

PREVIOUS WORK

Hallimondite was first mentioned by Walenta and Wimmenauer (1961) as a new lead uranyl arsenate hydrate. Walenta (1965) provided a formal description of hallimondite using material from the type locality of the Michael mine, near Reichenbach, east of Lahr in the Black Forest, Baden-Württemberg, Federal Republic of Germany. He reported morphologic data, physical and optical properties, synthesis methods, the formula $Pb_2(UO_2)(AsO_4)_2$, and the following crystallographic data: triclinic, space group $P\bar{1}$, $a = 7.123(11)$, $b = 10.469(16)$, $c = 6.844(10)$ Å, $\alpha = 100.57(17)°$, $\beta = 94.80(17)°$, $\gamma = 91.27(17)°$, $V = 499.6$ Å^3, $Z = 2$, $D_{meas} = 6.39$ g/cm^3, $D_{calc} = 6.40$ g/cm^3. In addition to the Reichenbach locality, hallimondite has been found in uranium mineralization at Buehlskopf, near Ellweiler, Federal Republic of Germany (Bültemann 1970).

The unit-cell dimensions of hallimondite are larger than those

*E-mail: andrewl@rom.on.ca

of parsonsite, consistent with the replacement of P by the larger As cation: $^{[4]}As^{5+}$ radius = 0.335 Å, $^{[4]}P^{5+}$ radius = 0.17 Å (Shannon 1976), and the α and β angles of the two minerals are similar. However, the γ interaxial angle reported by Walenta (1965), 91.27°, is not similar to that of parsonsite, γ ~86.3° (Vochten et al. 1991; Burns 2000; Table 1), and is not in good agreement with the data for hallimondite presented in this work, γ = 86.651(3)° (Table 1). It is possible that this lack of agreement stems from a typographical error in Walenta (1965) in which the interaxial angle γ has been reversed with its reciprocal space counterpart, γ*. If so, then the data of Walenta (1965) yield: γ = 87.80(17)°, V = 499.8 Å^3, and D_{calc} = 6.39 g/cm^3, on an anhydrous basis.

The structure of natural parsonsite, $Pb_2[(UO_2)(PO_4)_2]$, was determined by Burns (2000), who found no evidence of structural water, in contrast to the results of the bulk chemical analyses of natural parsonsite of Schoep (1923, 1930): $Pb_2[(UO_2)(PO_4)_2](H_2O)$, and Frondel (1950): $Pb_2[(UO_2)(PO_4)_2](H_2O)_2$, and the thermogravimetric results of Vochten et al. (1991) for synthetic parsonsite: $Pb_2[(UO_2)(PO_4)_2](H_2O)_{0.5}$. We have examined synthetic hallimondite and synthetic parsonsite to elucidate the role of water molecules in this structure type.

Experimental methods

Crystal synthesis

Crystals of synthetic hallimondite and parsonsite were obtained by mild hydrothermal methods, in which reactants were weighed into 23 mL Teflon-lined Parr acid digestion vessels and heated in Fisher Isotemp ovens. After reaction, the vessels were allowed to cool in air to room temperature. Synthesis of hallimondite was based on the method of Walenta (1965), and entailed reaction of 0.1012 g $UO_2(NO_3)_2(H_2O)_6$ (Strem), 0.1515 g $Pb(CH_3COO)_2(H_2O)_3$ (Aldrich), 0.1191 g $H_5As_3O_{10}$ (prepared by the method of Walton 1948), and 6 mL of ultrapure H_2O; the reactants were held at 180(1)°C for 7 days. Synthesis of parsonsite was considerably modified from the methods of Ross (1956) and Vochten et al. (1991), and involved 0.1126 g of fluorapatite [ideally $Ca_5(PO_4)_3F$, from the Liscombe Deposit, near Wilberforce, Ontario, Canada], 0.1528 g $Pb(NO_3)_2$ (Baker), 0.0999 g $UO_2(NO_3)_2(H_2O)_6$ (Strem), 0.1554 g concentrated HNO_3 (Fisher), and 6 mL of ultrapure H_2O; the reactants were held at 80(1)°C for 14 days.

Single-crystal X-ray diffraction

For both compounds, a suitable crystal was mounted on a Bruker Platform three-circle X-ray diffractometer operated at 50 keV and 40 mA, equipped with a 4K APEX CCD detector and a crystal-to-detector distance of ~4.7 cm. A sphere of three-dimensional data was collected for each crystal at room temperature using graphite-monochromatized Mo$K\alpha$ X-radiation and frame widths of 0.3° in ω. Details of the data acquisition and refinement parameters are provided in Table 1. The intensity data were reduced and corrected for Lorentz, polarization, and background effects using the program SAINT (Bruker 1998), and the unit-cell dimensions were refined using least-squares techniques. The lack of systematic absences of reflections for hallimondite and parsonsite were consistent with space groups $P1$ and $P\bar{1}$, and assigning phases to sets of normalized structure-factors gave mean values of $|E^2-1|$ of 0.954 and 0.939, respectively, consistent with $P\bar{1}$.

Scattering curves for neutral atoms, together with anomalous dispersion corrections, were taken from the *International Tables for X-ray Crystallography, Vol. C* (Wilson 1992). The SHELXTL Version 5 (Sheldrick 1998) series of programs was used for the solution and refinement of the crystal structures.

Structure solution and refinement

Both structures were refined on the basis of F^2 for all unique data, and included anisotropic displacement parameters for all atoms except those belonging to an H_2O group. In the final cycle of each refinement, the mean parameter shift/e.s.d. was 0.000. The structures of synthetic hallimondite and synthetic parsonsite were refined using the atomic positions of Burns (2000) for natural parsonsite as the starting model. The unit cells of hallimondite and parsonsite can be transformed to the conventional setting by the matrix $[001/\bar{1}00/0\bar{1}0]$; however, for ease of comparison to the previous literature, the original unconventional setting is used in this work.

Table 1. Crystallographic data and refinement parameters

Compound	Hallimondite	Parsonsite
a (Å)	7.1153(8)	6.8432(5)
b (Å)	10.4780(12)	10.4105(7)
c (Å)	6.8571(8)	6.6718(4)
α (°)	101.178(2)	101.418(1)
β (°)	95.711(3)	98.347(2)
γ (°)	86.651(3)	86.264(2)
V (Å^3)	498.64(3)	460.64(5)
Space group	$P1$	$P1$
Z	2	2
Formula	$Pb_2[(UO_2)(AsO_4)_2](H_2O)_{0.3}$	$Pb_2[(UO_2)(PO_4)_2]$
Formula weight	967.67	874.37
F(000)	810	732
μ (mm^{-1})	56.5	54.4
D_{calc} (g/mL)	6.445	6.304
Crystal size (mm)	0.10 × 0.04 × 0.03	0.11 × 0.11 × 0.03
Color and habit	yellow parallelepiped	yellow parallelepiped
Temperature (K)	293(2)	293(2)
Width (°), time (s)	0.3, 45	0.3, 10
Collection, hours	sphere, 35	sphere, 8
θ range	2.88–34.55°	3.01–34.47°
Data collected	$h \pm 11$, $k \pm 16$, $l \pm 10$	$h \pm 10$, $k \pm 16$, $l \pm 10$
Absorption*	SADABS	plate (001) 3°
Total refl.	10240	8471
Unique refl., R_{int}	4074, 0.036	3666, 0.067
Unique $\|F_o\| \geq 4\sigma_F$	3391	3181
Extinction	—	0.0018(2)
Parameters	141	142
$R1$† for $\|F_o\| \geq 4\sigma_F$	2.7	3.4
$R1$† all data, wR_2‡	3.4, 5.5	4.0, 7.6
Weighting a	0.0207	0.0210
Goodness of fit	0.933	1.004
Mean shift/e.s.d.	0.000	0.000
Peaks (e/Å^3)	2.6, −3.2	4.2, −3.0

* Corrections for absorption are either empirical, based on the intensities of equivalent reflections (program SADABS, G. Sheldrick, unpublished), or semi-empirical (crystal modelled as a plate, rejecting data within 3° of the primary X-ray beam).
† $R1 = [\Sigma||F_o| - |F_c||]/\Sigma|F_o| \times 100$.
‡ $wR_2 = [\Sigma[w(F_o^2 - F_c^2)^2]/\Sigma[w(F_o^2)^2]]^{0.5} \times 100$, $w = 1/(\sigma^2(F_o^2) + (a \cdot P)^2$, and $P = 1/3$ max$(0, F_o^2) + 2/3\ F_c^2$.

Following refinement of the hallimondite model, the second highest peak in the difference Fourier list (~2.49 e Å^{-3}) was located at interatomic distances from O8 (2.6 Å) and O9 (2.8 Å), consistent with O···O separations observed for hydrogen bonds (Jeffrey 1997). This peak was added to the hallimondite model as the oxygen atom O11 (Table 2); its site occupancy (Hawthorne et al. 1995), refined to 29(2)%, yielding the formula $Pb_2[(UO_2)(AsO_4)_2](H_2O)_{0.3}$.

Inspection of the final difference Fourier list of parsonsite revealed that only the twenty-sixth peak (~1.35 e Å^{-3}) was located at interatomic distances from O8 (2.5 Å) and O9 (2.9 Å), consistent with O···O separations observed for hydrogen bonds (Jeffrey 1997). However, the electron density of this site (at atomic coordinates 0,0,1/2) is below the resolution of the data set. Simultaneous refinement of the occupancy and displacement parameter, assuming the site corresponds to oxygen, yielded occupancy 6(2)% and U_{eq} = 0.07(5) Å^2, within 3σ of the experimental uncertainty, and consistent with a vacant position.

For hallimondite, the atomic positional parameters and displacement parameters are given in Table 2, and selected interatomic distances and angles are in Table 3. For parsonsite, atomic coordinates and displacement parameters are in Table 4, and interatomic distances are in Table 5. Bond valence sums at the cation and anion sites for the two compounds are in Tables 6 and 7, and were calculated using the parameters of Burns et al. (1997) for U^{6+}, Brown and Altermatt (1985) for P^{5+} and As^{5+}, and Krivovichev and Brown (2001) for Pb^{2+}. Structure factors for hallimondite and parsonsite are given in Tables 8 and 9 respectively.[1]

[1]For a copy of Tables 8 and 9, Document item AM-05-005, contact the Business Office of the Mineralogical Society of America (see inside front cover of recent issue) for price information. Deposit items may also be available on the American Mineralogist web site at http://www.minsocam.org.

TABLE 2. Atomic coordinates (×10⁴) and displacement parameters (Å² × 10³) for hallimondite

	x	*y*	*z*	U_{eq}	U_{11}	U_{22}	U_{33}	U_{23}	U_{13}	U_{12}
U1	6186(1)	8400(1)	988(1)	10(1)	16(1)	7(1)	8(1)	1(1)	3(1)	1(1)
Pb1	3090(1)	5416(1)	2785(1)	16(1)	18(1)	19(1)	12(1)	2(1)	3(1)	−1(1)
Pb2	451(1)	7776(1)	7170(1)	18(1)	21(1)	12(1)	22(1)	0(1)	6(1)	1(1)
As1	5365(1)	8167(1)	6206(1)	9(1)	13(1)	7(1)	7(1)	0(1)	2(1)	0(1)
As2	8238(1)	5494(1)	2763(1)	10(1)	11(1)	9(1)	9(1)	2(1)	1(1)	1(1)
O1	10022(6)	6340(5)	4155(6)	18(1)	12(2)	22(2)	18(2)	0(2)	−2(2)	−5(2)
O2	3486(6)	4738(4)	5851(6)	14(1)	13(2)	19(2)	13(2)	7(2)	5(2)	0(2)
O3	3859(6)	7840(5)	731(7)	21(1)	19(2)	25(3)	19(2)	5(2)	2(2)	−4(2)
O4	6811(6)	7288(4)	7623(6)	15(1)	22(2)	15(2)	7(2)	2(2)	0(2)	3(2)
O5	7149(7)	6298(4)	1057(6)	20(1)	34(3)	11(2)	13(2)	4(2)	−1(2)	6(2)
O6	3323(6)	7477(4)	5346(6)	17(1)	14(2)	17(2)	17(2)	−3(2)	2(2)	−4(2)
O7	5018(7)	540(4)	1927(6)	19(1)	40(3)	9(2)	8(2)	1(2)	2(2)	8(2)
O8	8504(6)	8978(5)	1144(7)	21(1)	22(2)	22(3)	21(2)	2(2)	5(2)	−9(2)
O9	6524(6)	8562(5)	4429(6)	19(1)	22(2)	23(3)	13(2)	5(2)	4(2)	−2(2)
O10	9230(6)	4099(4)	1582(7)	21(1)	29(2)	14(2)	19(2)	2(2)	9(2)	9(2)
O11*	500(40)	9720(30)	4740(50)	73(11)						

Notes: U_{eq} is defined as one third of the trace of the orthogonalized U_{ij} tensor. The anisotropic displacement parameter exponent takes the form: $-2\pi^2 [h^2a^{*2} U_{11} + ... + 2 hka^* b^* U_{12}]$.
* Refined occupancy 29(2)%; site is separated from its symmetry equivalent by 0.95(5) Å.

Fourier transform infrared spectroscopy

Infrared absorbance spectra were collected for a 75 μm crystal (maximum dimension) of hallimondite and a 100 μm crystal of parsonsite over the range 650–4000 cm⁻¹ with a resolution of 4 cm⁻¹. A total of 120 scans were collected for each sample and each background using a SensIR IlluminatIR spectrometer with a diamond attenuated-total-reflectance (ATR) objective mounted on an Olympus BX51 microscope. Because of the high mean refractive indices of hallimondite (~1.90) and parsonsite (~1.85), corrections for effects due to the ATR would have been non-linear and were not applied. The raw FTIR spectra are shown in Figure 1.

DESCRIPTION OF THE STRUCTURES

Hallimondite is isostructural with parsonsite, whose structure was described by Burns (2000). In both structures, hexavalent uranium occurs as a uranyl pentagonal bipyramid, whose interatomic distances are in excellent agreement with expected bond lengths for this coordination environment (cf. Fig. 2 of Burns et al. 1997). The $O3_{ap}$-U1-$O8_{ap}$ bond angle in both hallimondite and parsonsite is 177.6° (Tables 3 and 5). This slight deviation from linearity is common in the pentagonal bipyramidal coordination of uranyl ions (cf. Fig. 6 of Burns et al. 1997). The uranyl polyhedra in hallimondite and in parsonsite share an edge, forming dimers that are linked by edge- and vertex-sharing tetrahedra (arsenate = hallimondite, phosphate = parsonsite) to form chains along [001] (Fig. 2). Dimers of pentagonal bipyramids are an uncommon structural motif in uranyl structures, but are known from the chain structures of some synthetic uranyl selenites: $Ca[(UO_2)(SeO_3)_2]$, $Sr[(UO_2)(SeO_3)_2]$ and $Sr[(UO_2)(SeO_3)_2](H_2O)_2$ (Almond et al. 2002; Almond and Albrecht-Schmitt 2004), and occur as isolated clusters in the structure of $UO_2(OH)Cl(H_2O)_2$ (Aberg 1969). Structures with the francevillite sheet-anion topology (Burns et al. 1996) also contain dimers of uranyl pentagonal bipyramids, which in turn share edges with dimers of other polyhedra of higher bond valence to form sheets. The best-known examples of these sheets are the vanadate minerals of the carnotite group, but other minerals (e.g., uranosphaerite $Bi(UO_2)O_2OH$) and synthetic compounds with this sheet-anion topology have been described (Hughes et al. 2003; Locock et al. 2004).

There are two symmetrically distinct Pb positions connecting the chains in hallimondite and parsonsite. The coordination environment of the Pb atoms is considered to consist of the entire first shell of surrounding anions. The Pb1 position is in tenfold coordination with a mean Pb1-O distance of 2.88 Å in hallimondite, and 2.81 Å in parsonsite (Fig. 2, Tables 3 and 5). The Pb2 site is in sevenfold coordination by the O atoms of the uranyl phosphate chain in parsonsite, with a mean Pb2-O distance of 2.74 Å (Table 5). In hallimondite, the Pb2 site has two further interatomic distances to the O11 site, yielding a mean Pb2-O distance of 2.85 Å (Fig. 2, Table 3).

TABLE 3. Selected interatomic distances (Å) and angles (°) for hallimondite

U1-O3	1.770(4)	As1-O6	1.664(4)
U1-O8	1.777(4)	As1-O9	1.665(4)
U1-O5	2.276(4)	As1-O4	1.699(4)
U1-O9	2.321(4)	As1-O7[e]	1.704(4)
U1-O7[a]	2.336(4)	<As1-O>	1.68
U1-O4[b]	2.446(4)		
U1-O7[c]	2.524(4)	As2-O5	1.674(4)
$<U1_{eq}-O>$	1.77	As2-O10	1.681(4)
$<U1_{ap}-O>$	2.38	As2-O2[e]	1.681(4)
<O3-U1-O8>	177.6(2)°	As2-O1	1.694(4)
		<As2-O>	1.68
Pb1-O2	2.333(4)		
Pb1-O6	2.507(4)	Pb2-O10[e]	2.281(4)
Pb1-O1[d]	2.528(4)	Pb2-O1[d]	2.314(4)
Pb1-O2[e]	2.528(4)	Pb2-O6	2.474(4)
Pb1-O4[e]	2.790(4)	Pb2-O4[d]	2.728(4)
Pb1-O5[c]	2.883(4)	Pb2-O11	2.87(3)
Pb1-O10[d]	3.111(5)	Pb2-O11[h]	3.16(3)
Pb1-O3	3.230(5)	Pb2-O8[f]	3.185(5)
Pb1-O10[c]	3.385(4)	Pb2-O3[g]	3.259(4)
Pb1-O5	3.467(5)	Pb2-O9[d]	3.363(4)
<Pb1-O>	2.88	<Pb2-O>	2.85

Notes: a = *x*, *y* + 1, *z*; b = *x*, *y*, *z* − 1; c = −*x* + 1, −*y* + 1, −*z*, d = *x* − 1, *y*, *z*; e = −*x* + 1, −*y* + 1, −*z* + 1; f = *x* − 1, *y*, *z* + 1; g = *x*, *y*, *z* + 1; h = −*x*, −*y* + 2, −*z* + 1.

The O11 site in hallimondite is located in the cavity between the uranyl arsenate chains and the Pb atoms. A difference-Fourier map plotted along [010] and centered on the special position at 0,0,1/2, (Fig. 3) reveals that the electron density is consistent with a split site. Refinement of the O11 atomic coordinates show that it is separated from its symmetry equivalent by 0.95(5) Å. The bond valence sum of the O11 position is 0.16 v.u., consistent with its assignment as a H_2O group.

Why does the H_2O group of the O11 site occupy a split site rather than the special position? Unconstrained refinement of the structural model for hallimondite with O11 placed at the special position 0,0,1/2 yields identical occupancy of 0.30(2)

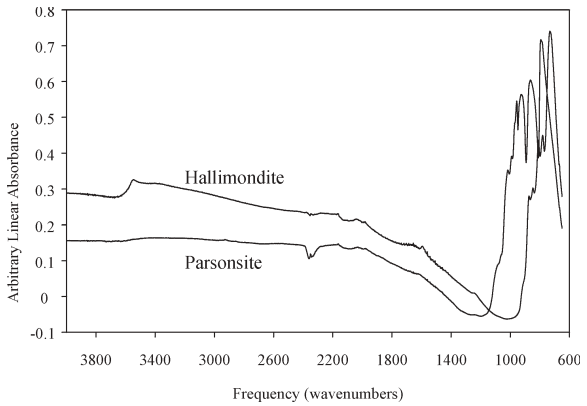

FIGURE 1. FTIR spectra of synthetic parsonsite and synthetic hallimondite. The peak at 3550 cm^{-1} in hallimondite corresponds to the O-H stretching mode, and the peak at 1590 cm^{-1} is the H_2O bending mode; these are absent in parsonsite. The peaks present between 600 and 1000 cm^{-1} correspond to vibrational modes of phosphate, arsenate and the uranyl ion. The glitches around 2300 cm^{-1} are due to the presence of CO_2 gas in the background measurement.

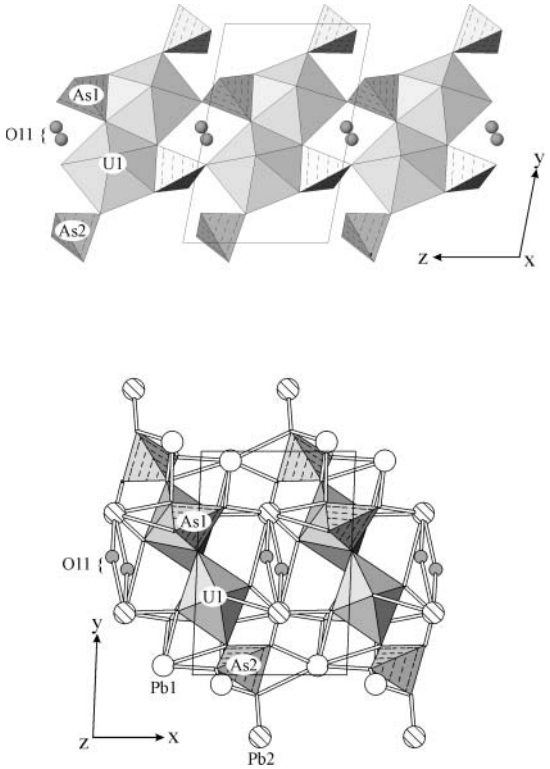

FIGURE 2. Upper: The structure of hallimondite, $Pb_2[(UO_2)(AsO_4)_2](H_2O)_{0.3}$, projected along [100]. The uranyl polyhedra are shown in gray and the arsenate tetrahedra are stippled. The H_2O groups are shown as small spheres, and the Pb atoms have been omitted for clarity. Lower: The structure of hallimondite projected along [001]. The Pb atoms are shown as large spheres: Pb1 is unfilled, and Pb2 is striped.

H_2O per formula unit, but the displacement parameter is considerably larger, U_{eq} = 0.15(2) $Å^2$, than in the split-site model, U_{eq} = 0.073(11) $Å^2$ (Table 2). The local environment of O11 is shown in Figure 4 for both the split site model and for O11

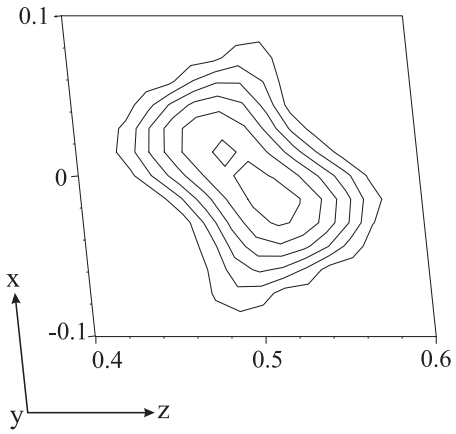

FIGURE 3. Difference Fourier map of the O11 position in hallimondite projected along [010]. The *x*- and *z*-axis scales are in fractions of the unit-cell dimensions. The contours start at 1.1 e/$Å^3$ with a contour interval of 0.2 e/$Å^3$.

fixed at the special position. In the split site model, the O···O separations are at somewhat more reasonable distances for hydrogen bonding, 2.72 and 2.80 Å, than if O11 is located at the special position, O···O distances 2.78 and 2.93 Å (Jeffrey 1997; Libowitzky 1999).

DISCUSSION

Hallimondite was originally described as an anhydrous mineral, $Pb_2[(UO_2)(AsO_4)_2]$, on the basis of microchemical and spectrographic analyses in which H_2O was not determined (Walenta 1965). However, our structure refinement is consistent with the presence of up to 0.5 H_2O per formula unit (pfu) in hallimondite, and this is supported by interpretation of the infrared absorbance spectrum (Fig. 1). Walenta (1965) noted that the optical behaviors of natural and synthetic hallimondite are not identical, and attributed this difference to radiation damage of the natural crystals. An alternative explanation is that the water content of hallimondite may be variable. In their discussion of the energetics of dehydration of zeolites, Bish and Carey (2001) recognize three types of water in zeolites, which can also be extended to mineral structures in general: (1) H_2O that varies in content as a continuous function of temperature and pressure (zeolitic H_2O), (2) H_2O that changes discontinuously at a unique temperature for a given pressure (hydrate H_2O), and (3) H_2O that is sorbed to external surfaces. Only zeolitic and hydrate H_2O are important from a structural point of view. In most hydrous uranyl phosphates and hydrous uranyl arsenates, water occurs as a hydrate H_2O, either coordinating interlayer cations, or occurring as interstitial H_2O groups. These H_2O groups participate in a hydrogen bond network that is necessary to maintain the integrity of the structure, e.g., structures of the autunite and meta-autunite groups (Locock and Burns 2003). In contrast, the presence of H_2O is probably not critical to the stability of the hallimondite structure, as no extensive hydrogen bond network is present. At maximum occupancy, O11 contributes only 0.12 v.u. to the bond valence sum of Pb2, regardless whether it is located at a split site or on the special position. In the current refinement, O11 is partly

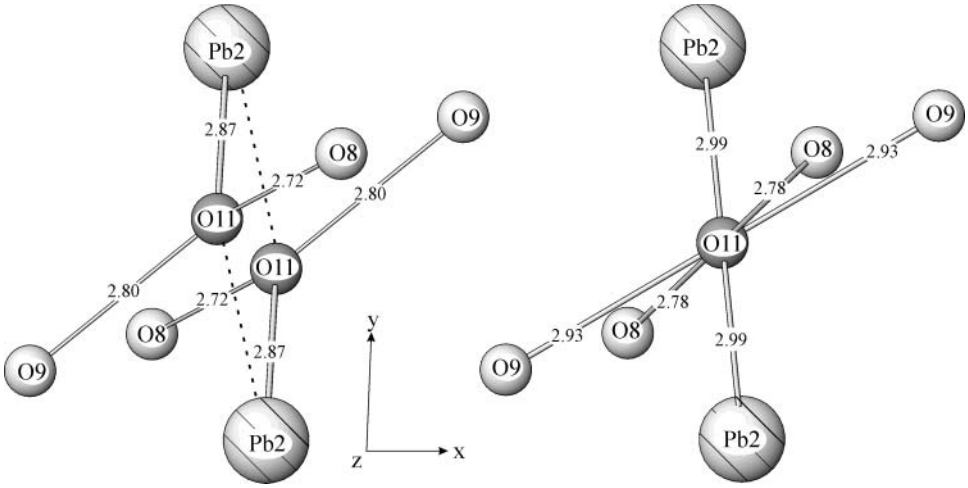

FIGURE 4. Local environment of the O11 position in hallimondite, projected along [001]. Left: Model with the O11 site split off the special position; dashed lines indicate Pb2-O11 bonds of 3.16 Å. Right: Model with the O11 atom on the special position with atomic coordinates 0,0,1/2. Interatomic distances are in angstroms.

TABLE 4. Atomic coordinates ($\times 10^4$) and displacement parameters ($Å^2 \times 10^3$) for parsonite

	x	*y*	*z*	U_{eq}	U_{11}	U_{22}	U_{33}	U_{23}	U_{13}	U_{12}
U1	6163(1)	8401(1)	1140(1)	12(1)	16(1)	8(1)	11(1)	2(1)	3(1)	0(1)
Pb1	3010(1)	5450(1)	2703(1)	17(1)	18(1)	19(1)	14(1)	3(1)	3(1)	−1(1)
Pb2	457(1)	7735(1)	7226(1)	17(1)	19(1)	11(1)	20(1)	0(1)	4(1)	0(1)
P1	5348(3)	8178(2)	6329(3)	11(1)	14(1)	8(1)	10(1)	1(1)	2(1)	1(1)
P2	8156(3)	5490(2)	2778(3)	11(1)	12(1)	9(1)	12(1)	2(1)	1(1)	1(1)
O1	9827(8)	6338(6)	4061(9)	16(1)	19(3)	13(2)	16(3)	−1(2)	2(2)	−1(2)
O2	3352(8)	4808(6)	5929(9)	18(1)	18(3)	20(3)	17(3)	8(2)	3(2)	−2(2)
O3	3673(9)	7895(6)	765(9)	20(1)	19(3)	20(3)	22(3)	6(2)	2(2)	1(2)
O4	6695(9)	7313(6)	7665(8)	16(1)	24(3)	11(2)	13(2)	5(2)	4(2)	7(2)
O5	7018(9)	6219(6)	1158(8)	17(1)	26(3)	12(2)	13(2)	5(2)	1(2)	5(2)
O6	3402(8)	7547(6)	5399(9)	17(1)	15(3)	15(3)	21(3)	2(2)	2(2)	−3(2)
O7	5007(9)	597(6)	1997(9)	17(1)	28(3)	9(2)	15(2)	4(2)	8(2)	5(2)
O8	8608(9)	8934(7)	1421(10)	22(1)	18(3)	26(3)	23(3)	5(3)	1(2)	−4(2)
O9	6434(9)	8524(6)	4693(8)	17(1)	25(3)	15(3)	12(2)	4(2)	4(2)	−4(2)
O10	9147(8)	4231(6)	1644(9)	17(1)	17(3)	14(3)	21(3)	7(2)	4(2)	4(2)

Notes: U_{eq} is defined as one third of the trace of the orthogonalized U_{ij} tensor. The anisotropic displacement parameter exponent takes the form: $-2\pi^2 [h^2a^{*2} U_{11} + ... + 2 hka^* b^* U_{12}]$.

TABLE 5. Selected interatomic distances (Å) and angles (°) for parsonsite

U1-O8	1.770(6)	P1-O9	1.516(6)
U1-O3	1.784(6)	P1-O6	1.518(6)
U1-O5	2.311(6)	P1-O7[e]	1.551(6)
U1-O9	2.329(5)	P1-O4	1.557(6)
U1-O7[a]	2.358(6)	<P1-O>	1.54
U1-O4[b]	2.438(5)		
U1-O7[c]	2.525(6)	P2-O2[e]	1.520(6)
<$U1_{eq}$-O>	1.78	P2-O5	1.535(6)
<$U1_{ap}$-O>	2.39	P2-O1	1.539(6)
<O3-U1-O8>	177.6(3)°	P2-O10	1.546(6)
		<P2-O>	1.53
Pb1-O2	2.353(5)		
Pb1-O1[d]	2.530(6)	Pb2-O10[e]	2.304(6)
Pb1-O6	2.540(6)	Pb2-O1[d]	2.315(6)
Pb1-O2[e]	2.541(6)	Pb2-O6	2.481(6)
Pb1-O5[c]	2.806(6)	Pb2-O4[d]	2.706(6)
Pb1-O4[e]	2.835(6)	Pb2-O3[f]	2.971(6)
Pb1-O10[d]	2.939(6)	Pb2-O9[d]	3.164(6)
Pb1-O10[c]	3.126(6)	Pb2-O8[g]	3.230(6)
Pb1-O3	3.159(6)	<Pb2-O>	2.74
Pb1-O5	3.265(6)		
<Pb1-O>	2.81		

Notes: a = *x*, *y* + 1, *z*; b = *x*, *y*, *z* – 1; c = –*x* + 1, –*y* + 1, –*z*; d = *x* – 1, *y*, *z*; e = –*x* + 1, –*y* + 1, –*z* + 1; f = *x*, *y*, *z* + 1 g = *x*–1, *y*, *z* + 1.

TABLE 6. Bond-valence analysis for synthetic hallimondite (v.u.)

	U1	Pb1	Pb2	As1	As2	Total
O1		0.316	0.489		1.218	2.02
O2		$0.316^{\downarrow}$, $0.470^{\downarrow\rightarrow}$			1.262	1.73
O3	1.715	0.075	0.071			1.86
O4	0.456	0.185	0.210	1.202		2.05
O5	0.636	$0.046^{\downarrow}$, $0.153^{\downarrow\rightarrow}$			1.286	2.07
O6		0.329	0.352	1.321		2.00
O7	$0.391^{\downarrow}$, $0.565^{\downarrow\rightarrow}$			1.186		1.75
O8	1.691		0.083			1.77
O9	0.582		0.057	1.317		1.96
O10		$0.055^{\downarrow}$, $0.096^{\downarrow\rightarrow}$	0.523		1.262	1.88
O11			$0.087^{\downarrow}$, $0.157^{\downarrow\rightarrow}$			0.16
Total	6.04	2.04	1.86*	5.03	5.03	

Notes: The symbols $^{\downarrow}$ and $^{\rightarrow}$ indicate that summation is carried out only in the given directions.
*The bond valence contributions of O11 to Pb2 have been scaled for the 29(2)% occupancy of the O11 site

occupied, and it is conceivable that the H_2O content at this site could vary from 0 to 0.5 pfu in a fashion more similar to zeolite minerals than to other hydrated uranyl arsenates.

Although parsonsite was originally described as a hydrous mineral, structure refinements of both natural (Burns 2000) and synthetic material (this work) are not consistent with the presence of any occupied sites attributable to H_2O. In addition, the FTIR spectrum of synthetic parsonsite does not support the presence of H_2O in this compound (Fig. 1). The original chemical analyses of natural parsonsite reported by Schoep (1923, 1930) and Frondel (1950) were made using bulk material from which considerable quantities of remaining and insoluble mate-

TABLE 7. Bond-valence analysis for synthetic parsonsite (v.u.)

	U1	Pb1	Pb2	P1	P2	Total
O1		0.315	0.488		1.234	2.04
O2		$0.308^{\downarrow}$, $0.451^{\downarrow\rightarrow}$			1.299	1.75
O3	1.668	0.087	0.128			1.88
O4	0.463	0.169	0.220	1.177		2.03
O5	0.594	$0.070^{\downarrow}$, $0.179^{\downarrow\rightarrow}$			1.250	2.02
O6		0.308	0.348	1.307		1.96
O7	$0.390^{\downarrow}$, $0.542^{\downarrow\rightarrow}$			1.194		1.74
O8	1.715		0.075			1.79
O9	0.572		0.086	1.313		1.97
O10		$0.093^{\downarrow}$, $0.136^{\downarrow\rightarrow}$	0.499		1.212	1.85
Total	5.94	2.12	1.84	4.99	5.00	

Note: The symbols $^{\downarrow}$ and $^{\rightarrow}$ indicate that summation is carried out only in the given directions.

rial were deducted (8.25 and 5.64 wt%, respectively). In light of these impurities, the water contents associated with these analyses should not necessarily be attributed (or at least not in their entirety) to the structure of parsonsite. Similarly, the low density reported for parsonsite by Frondel (1950), 5.37 g/cm^3, was made "on a relatively compact aggregate" and is therefore of questionable accuracy.

Could parsonsite contain H_2O in a manner analogous to hallimondite? Vochten et al. (1991) reported 0.96 wt% H_2O in synthetic parsonsite based on thermogravimetric analysis, consistent with the formula $Pb_2[(UO_2)(PO_4)_2](H_2O)_{0.5}$, and noted continuous loss of H_2O with increasing temperature.

Even though FTIR spectroscopy has not revealed any H_2O in the synthetic parsonsite studied, and crystal structure refinements have not revealed any significant electron density in parsonsite at the position corresponding to the O11 site of hallimondite, it is possible that in other specimens of parsonsite this site is occupied (cf. Vochten et al. 1991). An oxygen atom located at atomic coordinates 0,0,1/2, in parsonsite would be separated from O8 by 2.50 Å, from O9 by 2.93 Å, and from Pb2 by 3.00 Å. Interatomic distances between oxygen atoms of 2.40 to 2.55 Å are consistent with strong O-H···O bonds, although their occurrence is uncommon (Jeffrey 1997; Libowitzky 1999). In the presence of H_2O at this site, the bond valence sum for Pb2 in parsonsite would increase by 0.12 v.u. to 1.96 v.u., remaining in good agreement with its expected formal valence.

An oxygen atom located at a split site in parsonsite (at the same coordinates as in hallimondite), would have minimum separation distances from O8 of 2.42 Å, from O9 of 2.67 Å, and from Pb2 of 2.90 Å. Although very short O···O interatomic distances are not unknown in hydrogen bonds, it appears more likely that the special position would be adopted in parsonsite as there is no compelling structural reason for such a strong hydrogen bond to be present.

Analysis of cavities in the structure of parsonsite, carried out with the program ATOMS 5.1 (Dowty 2000), reveals that the position centered at 0,0,1/2 is the only significant void in the structure, and thus this position is the only candidate for the presence of structural water. Because this cavity is large enough to contain H_2O, and based on the current FTIR spectrum and the thermogravimetric results of Vochten et al. (1991), it is suggested that the water content in parsonsite could be variable, and that the formula of parsonsite should be considered $Pb_2[(UO_2)(PO_4)_2](H_2O)_n$, analogous to hallimondite, $Pb_2[(UO_2)(AsO_4)_2](H_2O)_n$, with $0 \leq n \leq 0.5$ in each case.

ACKNOWLEDGMENTS

This research was supported by the Environmental Management Science Program of the Office of Science, U.S. Department of Energy, grants DE-FGO7-97ER14820 and DE-FGO7-02ER63489. A.J.L. thanks the Environmental Molecular Sciences Institute, University of Notre Dame, for a 2003 EMSI Fellowship, and the International Centre for Diffraction Data for a 2004 Ludo Frevel Crystallography Scholarship. The authors thank F. Pertlik and an anonymous reviewer for their comments, and associate editor S. Quartieri for handling the manuscript.

REFERENCES CITED

Aberg, M. (1969) The crystal structure of $(UO_2)_2(OH)_2Cl_2(H_2O)_4$. Acta Chemica Scandinavica, 23, 791–810.

Almond, P.M. and Albrecht-Schmitt, T.E. (2004) Hydrothermal synthesis and crystal chemistry of the new strontium uranyl selenites, $Sr[(UO_2)_3(SeO_3)_2O_2]\cdot 4H_2O$ and $Sr[UO_2(SeO_3)_2]$. American Mineralogist, 89, 976–980.

Almond, P.M., Peper, S.M., Bakker, E., and Albrecht-Schmitt, T.E. (2002) Variable dimensionality and new uranium oxide topologies in the alkaline-earth metal uranyl selenites $AE[(UO_2)(SeO_3)_2]$ (AE = Ca, Ba) and $Sr[(UO_2)(SeO_3)_2]\cdot 2H_2O$. Journal of Solid State Chemistry, 168, 358–366.

Bish, D.L. and Carey, J.W. (2001) Thermal behavior of natural zeolites. In D.L. Bish and D.W. Ming, Eds., Natural Zeolites: Occurrence, Properties, Applications, 45, 403–452. Reviews in Mineralogy and Geochemistry, Mineralogical Society of America, Washington, D.C.

Brown, I.D. and Altermatt, D. (1985) Bond-valence parameters obtained from a systematic analysis of the inorganic crystal structure database. Acta Crystallographica, B41, 244–247.

Bruker (1998) SAINT, V 5.01 program for reduction of data collected on Bruker AXS CCD area detector systems. Bruker Analytical X-ray Systems, Madison, Wisconsin.

Bültemann, H. (1970) Uranium deposit at Buehlskopf near Ellweiler. Aufschluss, Sonderband 19, 129–134.

Burns, P.C. (1999) The crystal chemistry of uranium. In P.C. Burns and R. Finch, Eds., Uranium: Mineralogy, Geochemistry and the Environment, 38, 23–90. Reviews in Mineralogy, Mineralogical Society of America, Washington, D.C.

——— (2000) A new uranyl phosphate chain in the structure of parsonsite. American Mineralogist, 85, 801–805.

Burns, P.C., Miller, M.L., and Ewing, R.C. (1996) U^{6+} minerals and inorganic phases: a comparison and hierarchy of crystal structures. Canadian Mineralogist, 34, 845–880.

Burns, P.C., Ewing, R.C., and Hawthorne, F.C. (1997) The crystal chemistry of hexavalent uranium: polyhedron geometries, bond-valence parameters, and polymerization of polyhedra. Canadian Mineralogist, 35, 1551–1570.

Dowty, E. (2000) ATOMS for Windows and Macintosh, version 5.1. Shape Software, Kingsport, Tennessee.

Frondel, C. (1950) Studies of uranium minerals. I. Parsonsite and randite. American Mineralogist, 35, 245–250.

Hawthorne, F.C., Ungaretti, L., and Oberti, R. (1995) Site populations in minerals: terminology and presentation of results of crystal structure refinement. Canadian Mineralogist, 33, 907–911.

Hughes, K.-A., Burns, P.C., and Kolitsch, U. (2003) The crystal structure and crystal chemistry of uranosphaerite, $Bi(UO_2)O_2OH$. Canadian Mineralogist, 41, 677–685.

Jeffrey, G.A. (1997) An Introduction to Hydrogen Bonding, 303 p. Oxford University Press, New York.

King, R.B. (2002) Some aspects of structure and bonding in binary and ternary uranium(VI) oxides. Chemistry of Materials, 14, 3628–3635.

Kolitsch, U. and Giester, G. (2001) Revision of the crystal structure of ulrichite, $CaCu^{2+}(UO_2)(PO_4)_2\cdot 4H_2O$. Mineralogical Magazine, 65, 717–724.

Krause, W., Effenberger, H., and Brandstätter, F. (1995) Orthowalpurgite, $(UO_2)Bi_4O_4(AsO_4)_2\cdot 2H_2O$, a new mineral from the Black Forest, Germany. European Journal of Mineralogy, 7, 1313–1324.

Krivovichev, S.V. and Brown, I.D.(2001) Are the compressive effects of encapsulation an artifact of the bond valence parameters? Zeitschrift für Kristallographie, 216, 245–247.

Libowitzky, E. (1999) Correlation of the O-H stretching frequencies and O-H···O hydrogen bond lengths in minerals. Monatshefte für Chemie, 130, 1047–1059.

Locock, A.J. and Burns, P.C. (2003) Crystal structures and synthesis of the copper members of the autunite and meta-autunite groups: torbernite, zeunerite, metatorbernite and metazeunerite. Canadian Mineralogist, 41, 489–502.

Locock, A.J., Skanthakumar, S., Burns, P.C., and Soderholm, L. (2004) Syntheses, structures, magnetic properties, and X-ray absorption spectra of carnotite-type uranyl chromium(V) oxides: $A[(UO_2)_2Cr_2O_8](H_2O)_n$ (A = K_2, Rb_2, Cs_2, Mg; n = 0, 4). Chemistry of Materials, 16, 1384–1390.

Mereiter, K. (1982) The crystal structure of walpurgite, $(UO_2)Bi_4O_4(AsO_4)_2\cdot 2H_2O$. Tschermaks Mineralogische und Petrographische Mitteilungen, 30,

129–139.
Piret, P. and Piret-Meunier, J. (1994) Structure de la seelite de Rabejac (France). European Journal of Mineralogy, 6, 673–677.
Ross, V. (1956) Studies of uranium minerals. XXII. Synthetic calcium and lead uranyl phosphate minerals. American Mineralogist, 41, 915–926.
Schoep, A. (1923) Sur la parsonsite, nouveau minéral radioactif. Comptes Rendus Hebdomadaires des Séances de L'Académie des Sciences, 176, 171–173.
——— (1930) Les minéraux du gîte uranifère du Katanga. Annales du Musée du Congo Belge, serie 1, tome 1, fascicule 2, p. 1–43.
Shannon, R.D. (1976) Revised effective ionic radii and systematic studies of interatomic distances in halides and chalcogenides. Acta Crystallographica, A32, 751–767.
Sheldrick, G.M. (1998) SHELXTL NT, V5.1 program suite for solution and refinement of crystal structures. Bruker Analytical X-ray Systems, Madison, Wisconsin.
Vochten, R., Van Haverbeke, L., and Van Springel, K. (1991) Transformation of chernikovite into parsonsite and the study of its solubility product. Neues Jahrbuch für Mineralogie Monatshefte, 551–558.
Walenta, K. (1965) Hallimondite, a new uranium mineral from the Michael Mine near Reichenbach (Black Forest, Germany). American Mineralogist, 50, 1143–1157.
Walenta, K. and Wimmenauer, W. (1961) Der Mineralbestand des Michaelganges im Weiler bei Lahr (Schwarzwald). Jahreshefte des Geologischen Landesamts in Baden-Wuerttemberg, 4, 7–37.
Walton, H.F. (1948) Inorganic Preparations, A Laboratory Manual, p. 143–144. Prentice-Hall Inc., New York.
Wilson, A.J.C. Ed. (1992) International Tables for X-ray Crystallography, Volume C. Kluwer Academic Press, Boston.

MANUSCRIPT RECEIVED MAY 10, 2004
MANUSCRIPT ACCEPTED JULY 23, 2004
MANUSCRIPT HANDLED BY SIMONA QUARTIERI